IEEE Access
Multidisciplinary | Rapid Review | Open Access Journal

Received December 20, 2018, accepted January 10, 2019, date of publication January 25, 2019, date of current version February 12, 2019.

Digital Object Identifier 10.1109/ACCESS.2019.2895102

Joint Estimation of DOA and TDOA of Multiple Reflections by Matrix Pencil in Mobile Communications

YU ZHENG AND YONGZHI YU

College of Information and Communication Engineering, Harbin Engineering University, Harbin 150001, China

Corresponding author: Yongzhi Yu (yuyongzhi@hrbeu.edu.cn)

This work was supported in part by the National Natural Science Foundation of China under Grant 61571146, and in part by the Fundamental Research Funds for the Central Universities under Grant HEUCFP201808.

ABSTRACT This paper presents the joint estimation of the direction of arrival (DOA) and the time difference of arrival (TDOA) for multipath signals, which is the central issue for mobile communications. The estimator decouples the multi-dimensional problem for realizing the high resolution of DOA and TDOA based on the matrix pencil method without the computation of the correlation matrix. First, the data are transformed into the frequency domain to deconvolution by the known channel model, which maps delays into phase shifts in the frequency domain. Then, a two-dimensional matrix pencil algorithm yields the joint DOA and TDOA estimation based on the double Vandermonde structure data obtained. A closed-form solution without searching is given with the DOA and TDOA of incidence that can be paired automatically without an additional matching algorithm. The simulation results show that the proposed algorithm is not only suitable for the case that the elements' number is less than the source number but also for the case that multipath rays have equal DOA or TDOA.

INDEX TERMS Wireless communication, multipath signal, joint DOA/TDOA estimation, matrix pencil algorithms.

I. INTRODUCTION

Now wireless mobile communication era has arrived, increasing demand for higher data rate and quality of mobile communications leads to an evolution of mobile communication system [1], [2]. As one of the most popular research directions, the source localization is widely used in security and communication operations [3], [4]. On the one hand, it can be used to protect personal safety, such as playing an important role in the first aid location (like E-911 services). On the other hand, it will meet the requirements of wireless operation system in the future. In addition, the technology is also widely used in accident reporting, automatic billing, fraud detection, cargo tracking and intelligent transportation systems [5], [6]. In general, as the signal from the User Equipment(UE) to base station undergoes multipath rays of the direct signal, the multipath signals with different DOA and time delay combined with direct signal will degrade and influence the estimation of the desired signal. Therefore, in multipath environment, the DOA and time delay estimation on each path of user signal play a decisive part in the source localization.

The associate editor coordinating the review of this manuscript and approving it for publication was Liangtian Wan.

We mainly studied the joint DOA and time delay estimation of the signal transmitted by a single source through the multipath propagation. The method proposed in [7] and [8] require the known transmit signal to estimate angle and time delay. In [9], a method where Multiple Signal Classification (MUSIC) algorithm and cross correlation technique were used to estimate DOA and TDOA respectively is proposed, it considers multipath signals as independent signals. And in [10], a high resolution space-time joint estimation method is proposed, but it can't match automatically. Van der veen *et al.* have done a lot of works in the estimation method based on the parameter subspace. They realized the joint estimation of angle and time delay after the Fourier transform of the channel using the rotation invariance principle. Compared with the spectral estimation method represented by JADE-MUSIC [11], the computation of the JADE-ESPRIT [12] reduce greatly, because the angle and time delay can be directly solved without searching eigenvalue. However, since the Khatri-Rao product is introduced, the JADE-ESPRIT algorithm is still more complex than the one dimensional ESPRIT algorithm [13].

In this paper, a kind of matrix pencil algorithm [14] for harmonic recovery is proposed to estimate the DOA and

time delay. To introduce the matrix pencil method into channel parameter estimation, the channel response is estimated by least square (LS) method firstly. Then the time delay popular matrix was mapped into a matrix with Vandermond structure by Fourier transform. Finally, poles that contain DOA and TDOA information can be extracted by 2-D matrix pencil algorithm. There are some major advantages of the proposed algorithm compared with other high resolution parameter estimation methods. Firstly, the algorithm is simple and not limited by the coherent sources. Secondly, the algorithm is closed form and computationally attractive, in which DOA and TDOA can be estimated simultaneously without additional pairing algorithm. Finally, the algorithm can be used to estimate the source efficiently when the number of multipath is larger than the number of antenna array and adopt the requirements with few snapshots.

The rest of the paper is organized as follows: In Section II, the data model and channel model are presented. Section III contains a detailed derivation of the basic steps of the MP algorithm, and some processing techniques are readily incorporated into the algorithm to improve the estimation accuracy. Section IV illustrates the performance of the algorithm using computer simulations.

Notation: Vectors and matrices are denoted by boldface lower uppercase and uppercase boldface letters, respectively. Super-scripts $(\cdot)^T$, $(\cdot)^{(c)}$, $(\cdot)^H$, $(\cdot)^\dagger$ represent transpose, complex conjugate, complex conjugate transpose and Pseudo-inverse respectively. $\lceil\cdot\rceil$ and $\lfloor\cdot\rfloor$ are the ceiling and flooring of a decimal number respectively. Additionally, the symbol rank($\boldsymbol{Z}$) and $\boldsymbol{Z}_{a,b}$ denotes the rank of a matrix $\boldsymbol{Z}$ and the entry in the $(a+1)$-th row and $(b+1)$-th column of $\boldsymbol{Z}$.

II. DATA MODEL AND CHANNEL ESTIMATION

A. DATA MODEL

Considering that a user signal transmits a digital sequences $\{s_l\}$ over a mirror multipath environment and these digital sequences are received through a convolution channel by a uniform linear array(ULA) composed of M sensors in a base station. The distance between adjacent antenna elements is equal to half wavelength d, as shown in Fig.1. The receive date model of the array without noise can be expressed as the convolution of the digital sequence and the channel response, as follows:

$$\boldsymbol{x}(t) = \begin{bmatrix} x_1(t) \\ \vdots \\ x_M(t) \end{bmatrix} = \sum_l s_l \boldsymbol{h}(t - lT_s) \tag{1}$$

where T_s is the symbol period which is normalized to 1 for convenience. And the channel response $\boldsymbol{h}(t)$ comprising K radiation paths can be written as

$$\boldsymbol{h}(t) = \sum_{k=1}^{K} \boldsymbol{a}(\alpha_k)\beta_k g(t - \tau_k) \tag{2}$$

where α_k is DOA, β_k is complex fading coefficient, τ_k is time delay, and $g(t)$ is a known pulse shape function, which

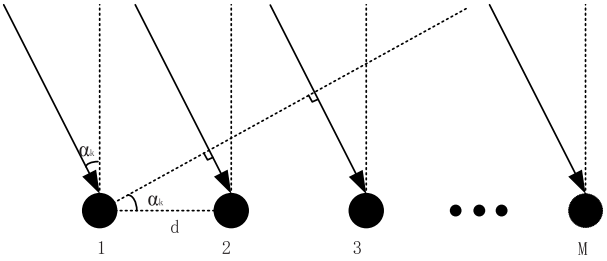

FIGURE 1. Schematic diagram of an antenna array with one impinging signal.

includes all the filtering at transmitter and receiver (the raised cosine pulse shape, as shown in Fig.2, is used here). The signal $\{s_l\}$ is modulated by $g(t)$. $\boldsymbol{a}(\alpha_k)$ is a $M \times 1$ steering vector for the array toward direction α_k expressed as

$$\boldsymbol{a}(\alpha_k) = [\,1 \quad \theta_k \quad \cdots \quad \theta_k{}^{M-1}\,]^T \tag{3}$$

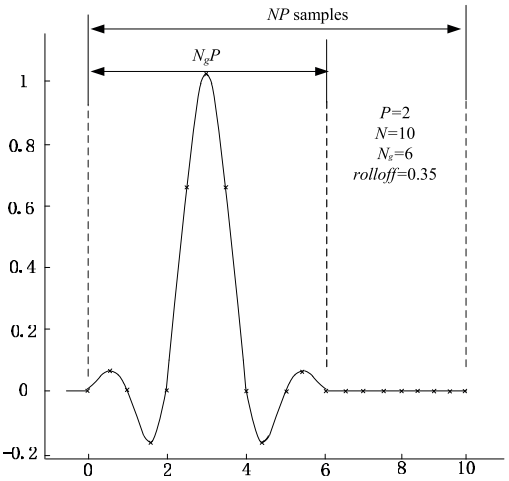

FIGURE 2. The raised cosine pulse shape function.

where $\theta_k = e^{j2\pi f_c d \sin(\alpha_k)/c}$, and f_c is carrier frequency, c represents the speed of light. Suppose that $g(t)$ is non-zero only in a finite interval $[0, N_g)$ so that $N = N_g + \tau_{\max}$ is finite, where N is the channel length measured in symbol periods and $\tau_{\max} = \lceil \max(\tau_k) \rceil$. Assuming that the received date $\boldsymbol{x}(t)$ is over sampled at the rate of P times symbol rate and collect a batch of L samples. If we stack the received date element $\boldsymbol{x}(\cdot)$ together every P samples, an $MP \times L$ matrix $\bar{\boldsymbol{X}}$ can be obtained as

$$\begin{aligned} \bar{\boldsymbol{X}} &= \begin{bmatrix} \bar{\boldsymbol{x}}_0 & \cdots & \bar{\boldsymbol{x}}_{L-1} \end{bmatrix} \\ &= \begin{bmatrix} \boldsymbol{x}(0) & \boldsymbol{x}(1) & \cdots & \boldsymbol{x}(L-1) \\ \boldsymbol{x}(\frac{1}{P}) & \boldsymbol{x}(1+\frac{1}{P}) & \cdots & \boldsymbol{x}(L-1+\frac{1}{P}) \\ \vdots & \vdots & & \vdots \\ \boldsymbol{x}(\frac{P-1}{P}) & \boldsymbol{x}(1+\frac{P-1}{P}) & \cdots & \boldsymbol{x}(L-1+\frac{P-1}{P}) \end{bmatrix} \end{aligned} \tag{4}$$

where $\bar{\boldsymbol{x}}_i = \left[(\boldsymbol{x}(i))^T \left(\boldsymbol{x}(i+\frac{1}{P})\right)^T \cdots \left(\boldsymbol{x}(i+\frac{P-1}{P})\right)^T \right]^T$

Based on Finite Impulse Response (FIR) assumption [12], $\bar{\boldsymbol{X}}$ has the following form

$$\bar{\boldsymbol{X}} = \bar{\boldsymbol{H}}\bar{\boldsymbol{S}} \tag{5}$$

where $\bar{\boldsymbol{H}}$ is an $MP \times N$ channel response matrix and $\bar{S}$ is a $N \times L$ Toeplitz matrix of the date symbols

$$\bar{\boldsymbol{H}} = \begin{bmatrix} \boldsymbol{h}(0) & \boldsymbol{h}(1) & \cdots & \boldsymbol{h}(N-1) \\ \boldsymbol{h}(\frac{1}{P}) & \boldsymbol{h}(1+\frac{1}{P}) & \cdots & \boldsymbol{h}(N-1+\frac{1}{P}) \\ \vdots & \vdots & & \vdots \\ \boldsymbol{h}(\frac{P-1}{P}) & \boldsymbol{h}(1+\frac{P-1}{P}) & \cdots & \boldsymbol{h}(N-1+\frac{P-1}{P}) \end{bmatrix}$$

$$\bar{\boldsymbol{S}} = \begin{bmatrix} s_0 & s_1 & \cdots & s_{L-1} \\ s_{-1} & s_0 & \cdots & s_{L-2} \\ \vdots & \vdots & & \vdots \\ s_{-N+1} & s_{-N+2} & \cdots & s_{L-N} \end{bmatrix}.$$

In the case that s_l is a known sequence, the channel response matrix can be estimated by using LS method

$$\bar{\boldsymbol{H}}_{est} = \bar{\boldsymbol{X}}\bar{\boldsymbol{S}}^{\dagger}. \tag{6}$$

After obtaining the estimated channel matrix $\bar{\boldsymbol{H}}_{est}$, it will be convenient to rearrange $\bar{\boldsymbol{H}}_{est}$ into a $M \times NP$ matrix

$$\boldsymbol{H} = [\boldsymbol{h}(0), \boldsymbol{h}(\frac{1}{P}), \cdots, \boldsymbol{h}(N-\frac{1}{P})]. \tag{7}$$

According to equation (2), H meets the following decomposition:

$$\begin{aligned} \boldsymbol{H} &= [\boldsymbol{a}(\alpha_1)\cdots\boldsymbol{a}(\alpha_K)] \begin{bmatrix} \beta_1 & & 0 \\ & \ddots & \\ 0 & & \beta_K \end{bmatrix} \begin{bmatrix} \boldsymbol{g}(\tau_1) \\ \vdots \\ \boldsymbol{g}(\tau_K) \end{bmatrix} \\ &= \boldsymbol{ABG} \end{aligned} \tag{8}$$

where $\boldsymbol{g}(\tau_i) = [\, g(0-\tau_i)\ g(\frac{1}{P}-\tau_i) \cdots g(N-\frac{1}{P}-\tau_i)\,]$ is a NP-dimensional sample row vector of $\boldsymbol{g}(t-\tau_i)$.

B. CHANNEL MODEL TRANSFORMATION

Fourier transform by which the variation of time delay can be transformed into the phase shift is used to estimate the time delay. The specific approach is by doing the Fourier transform to each row of the matrix $\boldsymbol{H}$. According to (8), the Fourier transform for each row of $\boldsymbol{H}$ is equal to the Fourier transform for each row of $\boldsymbol{G}$, which map the time delay into a matrix with Vandermonde structure. The Fourier transform of (8) by rows, we have

$$\boldsymbol{H}_f = \mathrm{DFT}[\boldsymbol{H}] = \boldsymbol{ABF}_{NP}\mathrm{diag}(\tilde{\boldsymbol{g}}) \tag{9}$$

where $\boldsymbol{F}_{NP}$ is the Vandermonde matrix

$$\boldsymbol{F}_{NP} = \begin{bmatrix} 1 & \phi_1 & \phi_1^2 & \cdots & \phi_1^{NP-1} \\ \vdots & \vdots & \vdots & \vdots & \vdots \\ 1 & \phi_K & \phi_K^2 & \cdots & \phi_K^{NP-1} \end{bmatrix}$$

and $\phi_k = e^{-j2\pi\tau_k/N}$, $\tilde{\boldsymbol{g}} = \mathrm{DFT}[\boldsymbol{g}(0)]$. The effect of the known channel shape function can be removed in the frequency domain by dividing $\boldsymbol{H}_f$ by diag $(\tilde{\boldsymbol{g}})$ if $\tilde{\boldsymbol{g}}$ is nonzero [12]. For a raised-cosine pulse shape with roll-off factor ρ that used here, the normalized bandwidth is $W_{\max} = 1+\rho$. Assuming that $W_{\max} < P$, then $\tilde{\boldsymbol{g}}$ has at most $NW_{\max}$ nonzero entries. To ignore the smaller values at the border, we set $W = 1$, and select only N the center frequency sample. For later use, we require that the selected frequencies appear in increasing order, which means the final half samples of $\tilde{\boldsymbol{g}}$ should be moved up to front. So an $NP \times NW$ selection matrix $\boldsymbol{J}_{\tilde{g}}$ is constructed as follows:

$$\boldsymbol{J}_{\tilde{g}} = \begin{bmatrix} 0 & \boldsymbol{I}_{\lfloor NW/2 \rfloor} \\ 0 & 0 \\ \boldsymbol{I}_{\lceil NW/2 \rceil} & 0 \end{bmatrix}_{NP \times NW}$$

If all entries are nonzero, we can factor $\mathrm{diag}(\tilde{\boldsymbol{g}}\boldsymbol{J}_{\tilde{g}})$ out of $\boldsymbol{H}_f\boldsymbol{J}_{\tilde{g}}$ and obtain

$$\tilde{\boldsymbol{H}} = \boldsymbol{H}_f\boldsymbol{J}_{\tilde{g}}\{\mathrm{diag}(\tilde{\boldsymbol{g}}\boldsymbol{J}_{\tilde{g}})\}^{-1} \tag{10}$$

which satisfies the model

$$\tilde{\boldsymbol{H}} = \boldsymbol{ABF} \tag{11}$$

where $\boldsymbol{F}$ is a $K \times N$ Vandermonde matrix like $\boldsymbol{F}_{NP}$.

III. JOINT DOA AND TDOA ESTIMATION

Using the model $\tilde{\boldsymbol{H}} = \boldsymbol{ABF}$, we can estimate (α_k, τ_k), which are the functions of ϕ_k and θ_k, respectively. According to the literature [15], ϕ_k and θ_k can be approximated as the multipath model poles. Therefore, our problem becomes to calculate the pair of poles with the information of DOA and time delay respectively.

A. MATRIX PENCIL ALGORITHM

Based on the channel model obtained in (11), the elements in the first row of matrix $\tilde{\boldsymbol{H}}$ can be described by

$$\tilde{H}_{0,n} = \sum_{k=1}^{K} \beta_k \phi_k^n, \quad n = 0, 1 \ldots, N-1. \tag{12}$$

The matrix pencil method is based on the property of the exponential operation and it begins by setting a pencil parameter z_1, which can be selected in the range $K \le z_1 \le N-K$ [14]. Then define a new matrix $\boldsymbol{Y}_0$ as

$$\boldsymbol{Y}_0 = \begin{bmatrix} H_{0,0} & H_{0,1} & \cdots & H_{0,N-z_1} \\ H_{0,1} & H_{0,2} & \cdots & H_{0,N-z_1+1} \\ \vdots & \vdots & \ddots & \vdots \\ H_{0,z_1-1} & H_{0,z_1} & \cdots & H_{0,N-1} \end{bmatrix}. \tag{13}$$

Two matrices $\boldsymbol{Y}_L$ and $\boldsymbol{Y}_R$ present the first z_1-1 rows and the last z_1-1 rows of the matrix $\boldsymbol{Y}_0$, respectively. According to the definition of matrix pencil, it is a linear combination of the two matrices and a scalar λ, $\boldsymbol{Y}_R - \lambda\boldsymbol{Y}_L$. In the noiseless case, it is easy to verify that $\boldsymbol{Y}_L$ and $\boldsymbol{Y}_R$ can be decomposed as follows:

$$\begin{aligned} \boldsymbol{Y}_L &= \boldsymbol{Z}_{L1}\boldsymbol{B}\boldsymbol{Z}_R \\ \boldsymbol{Y}_R &= \boldsymbol{Z}_{L2}\boldsymbol{B}\boldsymbol{Z}_R = \boldsymbol{Z}_{L1}\boldsymbol{\Gamma}(\phi)\boldsymbol{B}\boldsymbol{Z}_R \end{aligned} \tag{14}$$

where $\mathbf{\Gamma}(\phi) = \text{diag}[\phi_1, \phi_2, \ldots, \phi_K]$, $\mathbf{Z}_{L1}$ and $\mathbf{Z}_{L2}$ are the first $z_1 - 1$ rows and the last $z_1 - 1$ rows of the following matrix

$$\mathbf{Z}_L = \begin{bmatrix} 1 & 1 & \cdots & 1 \\ \phi_1 & \phi_2 & \cdots & \phi_K \\ \vdots & \vdots & \cdots & \\ \phi_1^{z_1-1} & \phi_2^{z_1-1} & \cdots & \phi_K^{z_1-1} \end{bmatrix} \tag{15}$$

and

$$\mathbf{Z}_R = \begin{bmatrix} 1 & \phi_1 & \cdots & \phi_1^{N-z_1} \\ 1 & \phi_2 & \cdots & \phi_2^{N-z_1} \\ \vdots & \vdots & & \vdots \\ 1 & \phi_K & \cdots & \phi_K^{N-z_1} \end{bmatrix}. \tag{16}$$

The expression of the matrix pencil can be further written as:

$$\boldsymbol{Y}_R - \lambda \boldsymbol{Y}_L = \boldsymbol{Z}_{L1} \left(\mathbf{\Gamma}(\phi) - \lambda \boldsymbol{I}\right) \boldsymbol{B} \boldsymbol{Z}_R \tag{17}$$

where $\boldsymbol{I}$ is a $K \times K$ unit matrix. Generally, the rank of $\boldsymbol{Y}_R - \lambda \boldsymbol{Y}_L$ is K. When $\lambda = \phi_k (k = 1, \cdots, K)$, the k-th row of $\mathbf{\Gamma}(\phi) - \lambda \boldsymbol{I}$ is equal to zero, and the rank of $Y_R - \lambda Y_L$ will be reduced by one. Based on the correlation principle of matrix pencil, the problem of solving the set of the poles $\{\phi_k, k = 1, \ldots, K\}$ becomes the generalized eigenvalue problem of solving matrix pair $(\boldsymbol{Y}_R, \boldsymbol{Y}_L)$.

Similarly, if we take the first column of the matrix $\tilde{\boldsymbol{H}}$ to construct the matrix $\boldsymbol{Y}_0$, then the estimation of the set of the poles $\{\theta_k, k = 1, \ldots, K\}$ can be also achieved according to the above principle.

B. ENHANCED MATRIX

From (11), we know that $\text{rank}(\tilde{\boldsymbol{H}}) \leq K$. In the condition of $M \geq K$ and $N \geq K$, it can be shown that $\tilde{\boldsymbol{H}}$ has the rank K if and only if the two sets of the 1-D poles $\{\phi_k, k = 1, \ldots, K\}$ and $\{\theta_k, k = 1, \ldots, K\}$ both contain distinct elements. That means the received rays have an equal DOA or time delay, $\tilde{\boldsymbol{H}}$ will become rank deficient. Once $\text{rank}(\tilde{\boldsymbol{H}})$ is less than K, the pole information $\{\phi_k, k = 1, \ldots, K\}$ and $\{\theta_k, k = 1, \ldots, K\}$ cannot be obtained simultaneously from the principal left and right singular vectors of $\tilde{\boldsymbol{H}}$. In addition, the principle singular vectors of $\tilde{\boldsymbol{H}}$ do not contain sufficient information to perform the pairing between θ_k and ϕ_k [16]. Therefore, we adopt the method of partition and stack to extend the rank of matrix.

The Hankel matrix $\boldsymbol{Y}_m$ stacked by elements of each line of $\tilde{\boldsymbol{H}}$ is given

$$\boldsymbol{Y}_m = \begin{bmatrix} H_{m,0} & H_{m,1} & \cdots & H_{m,N-z_1} \\ H_{m,1} & H_{m,2} & \cdots & H_{m,N-z_1+1} \\ \vdots & \vdots & \ddots & \vdots \\ H_{m,z_1-1} & H_{m,z_1} & \cdots & H_{m,N-1} \end{bmatrix}. \tag{18}$$

$\boldsymbol{Y}_m$ is a $z_1 \times (N - z_1 + 1)$ Hankel matrix. The augmented matrix Y_e, which is composed of matrix Y_m, can be further obtained

$$\boldsymbol{Y}_e = \begin{bmatrix} \boldsymbol{Y}_0 & \boldsymbol{Y}_1 & \cdots & \boldsymbol{Y}_{M-z_2} \\ \boldsymbol{Y}_1 & \boldsymbol{Y}_2 & \cdots & \boldsymbol{Y}_{M-z_2+1} \\ \vdots & \vdots & \ddots & \vdots \\ \boldsymbol{Y}_{z_2-1} & \boldsymbol{Y}_{z_2} & \cdots & \boldsymbol{Y}_{M-1} \end{bmatrix} \tag{19}$$

$\boldsymbol{Y}_e$ is a $z_1 z_2 \times (M - z_2 + 1)(N - z_1 + 1)$ Hankel block matrix and z_2 is also a pencil parameter to construct the Hankel matrix. The value of z_1 and z_2 effects on the accuracy of the estimation. Each column of $\boldsymbol{Y}_m$ can be consider as a segment of the sequence $[H_{m,0}, \cdots, H_{m,z_1-1}]$ with the window length z_1, and z_2 is the window length of the column $\boldsymbol{Y}_e$. So z_1 and z_2 can be considered as two tuning parameters.

According to the principle of matrix pencil [14], Y_m can be decomposed

$$\boldsymbol{Y}_m = \boldsymbol{Z}_L \boldsymbol{B} (\mathbf{\Gamma}(\theta))^m \boldsymbol{Z}_R \tag{20}$$

where $\mathbf{\Gamma}(\theta)$=diag$[\theta_1, \theta_2, \ldots, \theta_K]$. Substituting (20) into (19), the decomposition of Y_e can be written as:

$$\boldsymbol{Y}_e = \boldsymbol{D}_L \boldsymbol{B} \boldsymbol{D}_R, \tag{21}$$

where

$$\boldsymbol{D}_L = \begin{bmatrix} \boldsymbol{Z}_L{}^T & (\boldsymbol{Z}_L \mathbf{\Gamma}(\theta))^T & \cdots & (\boldsymbol{Z}_L (\mathbf{\Gamma}(\theta))^{z_2-1})^T \end{bmatrix}^T$$
$$\boldsymbol{D}_R = \begin{bmatrix} \boldsymbol{Z}_R & \Gamma(\theta) \boldsymbol{Z}_R & \cdots & (\mathbf{\Gamma}(\theta))^{M-z_2} \boldsymbol{Z}_R \end{bmatrix}$$

In order to guarantee $\text{rank}(\boldsymbol{Y}_e) = K$, $\text{rank}(\boldsymbol{D}_L) = \text{rank}(\boldsymbol{D}_R) = K$ is needed. So the value of z_1 and z_2 must meet certain requirements. Here, $\boldsymbol{D}_L$ is a $z_1 z_2 \times K$ dimensional matrix, and $\boldsymbol{D}_R$ is a $K \times (M - z_2 + 1)(N - z_1 + 1)$ dimensional matrix. So the necessary conditions for the full rank of the two matrices are

$$\begin{aligned} z_1 z_2 &\geq K \\ (M - z_2 + 1)(N - z_1 + 1) &\geq K. \end{aligned} \tag{22}$$

Based on the requirements that the poles ϕ_k and θ_k are all located in the unit circle and the centro-symmetric structures of $\boldsymbol{Y}_e$, a well-known technique called forward-backward averaging method is commonly used to further extend the matrix $\boldsymbol{Y}_{ex}$ which is defined as:

$$\begin{bmatrix} \boldsymbol{Y}_e & \mathbf{\Pi}_{z_1 z_2} \boldsymbol{Y}_e^{(c)} \mathbf{\Pi}_{(M-z_2+1)(N-z_1+1)} \end{bmatrix} \tag{23}$$

where $\mathbf{\Pi}_z$ is called the exchange matrix and defined as a $z \times z$ square matrix, i.e,

$$\mathbf{\Pi}_z = \begin{bmatrix} 0 & \cdots & 0 & 0 & 1 \\ 0 & \cdots & 0 & 1 & 0 \\ 0 & \cdots & 1 & 0 & 0 \\ \vdots & \ddots & \vdots & \vdots & \vdots \\ 1 & \cdots & 0 & 0 & 0 \end{bmatrix}_{z \times z}$$

C. RANK REDUCTION

As the existence of noise, the matrix $\boldsymbol{Y}_{ex}$ will be of full rank rather than rank K, so the technique of singular value decomposition (SVD) and QR decomposition can be used to reduce the matrix to size $K \times K$. The signal subspace Y_{ex} can be obtained through SVD

$$\boldsymbol{Y}_{ex} = \boldsymbol{U}\boldsymbol{\Sigma}\boldsymbol{V}^H = \boldsymbol{U}_s\boldsymbol{\Sigma}_s{\boldsymbol{V}_s}^H + \boldsymbol{U}_n\boldsymbol{\Sigma}_n{\boldsymbol{V}_n}^H \tag{24}$$

where $\boldsymbol{U}_s$ and $\boldsymbol{V}_s$ are the submatrix of $\boldsymbol{U}$ and $\boldsymbol{V}$, that corresponded to the singular values of $\boldsymbol{\Sigma}_s$ and span signal subspace. $\boldsymbol{U}_n$ and $\boldsymbol{V}_n$ are corresponded to the singular value of $\boldsymbol{\Sigma}_n$ and span noise subspace.

We define two special matrix $\boldsymbol{U}_{s1}$ and $\boldsymbol{U}_{s2}$, which are obtained by removing the last z_1 rows and the first z_1 rows of $\boldsymbol{U}_s$, respectively. A alternative way is to compute a QR factorization of $\boldsymbol{U}_{s1}$ and to apply the $\boldsymbol{Q}$ factor to $\boldsymbol{U}_{s2}$ as well, which corresponds to a LS projection of the column span of $\boldsymbol{U}_{s2}$ onto that of $\boldsymbol{U}_{s1}$.

$$\boldsymbol{Q}[\,\boldsymbol{U}_{s1} \quad \boldsymbol{U}_{s2}\,] = \begin{bmatrix} \boldsymbol{E}_{s1} & \boldsymbol{E}_{s2} \\ 0 & * \end{bmatrix}. \tag{25}$$

The original data matrices have now been reduced to equivalent data matrices. There exist certain nonsingular $K \times K$ matrices $\boldsymbol{S'}$ and $\boldsymbol{T}$ satisfying

$$\begin{cases} \boldsymbol{E}_{s1} = \boldsymbol{S'}\boldsymbol{T} \\ \boldsymbol{E}_{s2} = \boldsymbol{S'}\boldsymbol{\Gamma}(\theta)\boldsymbol{T} \end{cases}. \tag{26}$$

For further estimate ϕ_k, a shuffle matrix is introduced to rearrange the signal subspace as $\boldsymbol{U}_{sp} = \boldsymbol{P}_c\boldsymbol{U}_s$ [17], where $\boldsymbol{P}_c$ is defined as

$$\begin{aligned} \boldsymbol{P}_c = [&\boldsymbol{p}_c(1), \boldsymbol{p}_c(1+z_1), \ldots, \boldsymbol{p}_c(1+(z_2-1)z_1), \boldsymbol{p}_c(2), \\ &\boldsymbol{p}_c(2+z_1), \ldots, \boldsymbol{p}_c(2+(z_2-1)z_1), \ldots, \boldsymbol{p}_c(z_1), \\ &\boldsymbol{p}_c(z_1+z_1), \ldots, \boldsymbol{p}_c(z_1+(z_2-1)z_1)]^T \end{aligned}$$

where $\boldsymbol{p}_c(i)$ is the $z_2z_1 \times 1$ column vector, whose elements value are all zero except that the i-th element value is one. Then, the two special matrix of $\boldsymbol{U}_{sp1}$ and $\boldsymbol{U}_{sp2}$ can also be obtained by removing the last z_2 rows and the first z_2 rows of $\boldsymbol{U}_{sp}$, respectively. Computing a QR factorization of $\boldsymbol{U}_{sp1}$ and applying the $\boldsymbol{Q'}$ factor to $\boldsymbol{U}_{sp2}$, we have

$$\boldsymbol{Q'}[\,\boldsymbol{U}_{sp1} \quad \boldsymbol{U}_{sp2}\,] = \begin{bmatrix} \boldsymbol{E}_{sp1} & \boldsymbol{E}_{sp2} \\ 0 & * \end{bmatrix}. \tag{27}$$

Similarly, certain nonsingular $K \times K$ matrices $\boldsymbol{S''}$ can be obtained, which satisfy

$$\begin{cases} \boldsymbol{E}_{sp1} = \boldsymbol{S''}\boldsymbol{T} \\ \boldsymbol{E}_{sp2} = \boldsymbol{S''}\boldsymbol{\Gamma}(\phi)\boldsymbol{T} \end{cases} \tag{28}$$

D. EXTRACTING DOA AND TDOA

In the joint estimation of DOA and TDOA, a main problem in some conventional approach [8], [12], [17] is that these estimated delays cannot be associated with their respective DOAs. In other words, an additional pairing algorithm is needed, which will constitutes more computational expense. In this section, we will show a method to extract the pairs of θ_k and ϕ_k.

According to (26), a new matrix pencil function can be expressed into

$$\begin{aligned} \boldsymbol{E}_{s2} - \lambda\boldsymbol{E}_{s1} &= \boldsymbol{S'}(\boldsymbol{\Gamma}(\theta) - \lambda\boldsymbol{I})\boldsymbol{T} \\ \text{or} \quad (\boldsymbol{E}_{s2} - \lambda\boldsymbol{E}_{s1})w_k &= [\boldsymbol{S'}(\boldsymbol{\Gamma}(\theta) - \lambda\boldsymbol{I})\boldsymbol{T}]w_k = 0 \end{aligned} \tag{29}$$

where w_k is the generalized eigenvector of the matrix pencils $\boldsymbol{E}_{s2} - \lambda\boldsymbol{E}_{s1}$. Let $\boldsymbol{\Psi}_\theta{=}\boldsymbol{E}_{s1}^{\dagger}\boldsymbol{E}_{s2}$ and matrices $\boldsymbol{\Psi}_\theta$ satisfies

$$\boldsymbol{\Psi}_\theta{=}\boldsymbol{T}^{-1}\boldsymbol{\Gamma}(\theta)\boldsymbol{T}. \tag{30}$$

So the DOA of k-th path can be estimated as $\hat{\alpha}_k = \sin^{-1}((\angle\theta_k)c/2\pi f_c d)$. Then we will extract ϕ_k by using the generalized eigenvector w_k, which corresponds to $\hat{\alpha}_k$. Considering that it is possible to receive the rays with the same DOA and different TDOAs, so assuming that there are κ distinct eigenvalues in $\boldsymbol{\Gamma}(\theta)$ and the multiplicity of these eigenvalues is $r_i, i = 1, \ldots, \kappa$. If $r_i{=}1$, that is to say, the i-th eigenvalue is unique and the corresponding columns in $\boldsymbol{W} = [\boldsymbol{w}_1, \boldsymbol{w}_2, \cdots, \boldsymbol{w}_K]$ and $\boldsymbol{T}^{-1}$ are proportional. If $r_i > 1$, it means the i-th eigenvalue is repeated and the corresponding columns in $\boldsymbol{T}^{-1}$ are linear combination of those in W [18]. This relationship can be described by

$$\boldsymbol{W}\boldsymbol{R} = \boldsymbol{T}^{-1} \tag{31}$$

where R is a nonsingular block diagonal matrix as follows

$$\boldsymbol{R}{=}\begin{bmatrix} \boldsymbol{R}_1 & 0 & 0 & 0 \\ 0 & \boldsymbol{R}_2 & 0 & 0 \\ 0 & 0 & \ddots & 0 \\ 0 & 0 & 0 & \boldsymbol{R}_\kappa \end{bmatrix} \tag{32}$$

The submatrix $\boldsymbol{R}_i$, $i = 1, \ldots, \kappa$, corresponds to each distinct eigenvalue. If $r_i = 1$, $\boldsymbol{R}_i$ is a 1×1 identity matrix. If $r_i > 1$, $\boldsymbol{R}_i$ is a $r_i \times r_i$ nonsingular matrix.

Similar to (29), the second matrix pencil can be obtained to extract the poles ϕ_k as:

$$\begin{aligned} \boldsymbol{E}_{sp2} - \lambda\boldsymbol{E}_{sp1} &= \boldsymbol{S''}(\boldsymbol{\Gamma}(\phi) - \lambda\boldsymbol{I})T \\ \text{or} \quad (\boldsymbol{E}_{sp2} - \lambda\boldsymbol{E}_{sp1})\boldsymbol{\xi}_k &= [\boldsymbol{S''}(\boldsymbol{\Gamma}(\phi) - \lambda\boldsymbol{I})\boldsymbol{T}]\boldsymbol{\xi}_k = 0 \end{aligned} \tag{33}$$

where $\boldsymbol{\xi}_k$ is the generalized eigenvector of the matrix pencils $\boldsymbol{E}_{sp2} - \lambda\boldsymbol{E}_{sp1}$. Let $\boldsymbol{\Psi}_\phi{=}\boldsymbol{E}_{sp1}^{+}\boldsymbol{E}_{sp2}$, we can rewrite (33) as

$$\boldsymbol{\Psi}_\phi = \boldsymbol{\Xi}\boldsymbol{\Gamma}(\phi)\boldsymbol{\Xi}^{-1} \tag{34}$$

where $\boldsymbol{\Xi} = [\boldsymbol{\xi}_1, \boldsymbol{\xi}_2, \cdots, \boldsymbol{\xi}_K]$. Assuming that there are μ distinct eigenvalues in $\Gamma(\phi)$. Similar to (31), we have

$$\boldsymbol{\Xi}\boldsymbol{R'} = \boldsymbol{T}^{-1} \tag{35}$$

where $\boldsymbol{R'}$ is a block diagonal matrix as follows

$$\boldsymbol{R'}{=}\begin{bmatrix} \boldsymbol{R'}_1 & 0 & 0 & 0 \\ 0 & \boldsymbol{R'}_2 & 0 & 0 \\ 0 & 0 & \ddots & 0 \\ 0 & 0 & 0 & \boldsymbol{R'}_\mu \end{bmatrix} \tag{36}$$

Similarly, for $j = 1, \ldots, \mu$, if r_j=1, $\boldsymbol{R'}_j$ is a 1×1 identity matrix. If $r_j > 1$, $\boldsymbol{R'}_j$ is a $r_j \times r_j$ nonsingular matrix. According to (31) and (35), we have $\boldsymbol{W} = \boldsymbol{\Xi}\boldsymbol{R'}\boldsymbol{R}^{-1}$. If we premultiply $\boldsymbol{\Psi}_\phi$ with $\boldsymbol{W}^{-1}$ and postmultiply with $\boldsymbol{W}$, we can get

$$\boldsymbol{W}^{-1}\boldsymbol{\Psi}_\phi\boldsymbol{W} = \boldsymbol{R}\boldsymbol{R'}^{-1}\boldsymbol{\Gamma}(\phi)\boldsymbol{R'}\boldsymbol{R}^{-1} = \boldsymbol{R}\boldsymbol{\Gamma}(\phi)\boldsymbol{R}^{-1} \quad (37)$$

Because no matter whether ϕ_k is repeated or not, the diagonal elements with multiplicity r_j in $\boldsymbol{\Gamma}(\phi)$ correspond directly with the $r_j \times r_j$ nonsingular submatrix $\boldsymbol{R'}_j$. Thus, $\boldsymbol{\Gamma}(\phi)$ is commutative with respect to $\boldsymbol{R'}$ and $\boldsymbol{R'}^{-1}$. Then decomposing $\boldsymbol{\Gamma}(\phi)$ according to the the multiplicity of the eigenvalues in $\boldsymbol{\Gamma}(\theta)$ is

$$\boldsymbol{\Gamma}(\phi) = \begin{bmatrix} \bar{\boldsymbol{\phi}}_1 & 0 & 0 & 0 \\ 0 & \bar{\boldsymbol{\phi}}_2 & 0 & 0 \\ 0 & 0 & \ddots & 0 \\ 0 & 0 & 0 & \bar{\boldsymbol{\phi}}_\kappa \end{bmatrix}$$

In this way $\boldsymbol{R}_i$ and $\bar{\boldsymbol{\phi}}_i$ have the same size, then (37) can be further written as

$$\boldsymbol{R}\boldsymbol{\Gamma}(\phi)\boldsymbol{R}^{-1} = \begin{bmatrix} \boldsymbol{R}_1\bar{\boldsymbol{\phi}}_1\boldsymbol{R}_1^{-1} & 0 & 0 & 0 \\ 0 & \boldsymbol{R}_2\bar{\boldsymbol{\phi}}_2\boldsymbol{R}_2^{-1} & 0 & 0 \\ 0 & 0 & \ddots & 0 \\ 0 & 0 & 0 & \boldsymbol{R}_\kappa\bar{\boldsymbol{\phi}}_\kappa\boldsymbol{R}_\kappa^{-1} \end{bmatrix}$$

If the multiplicity of the eigenvalues in $\boldsymbol{\Gamma}(\theta)$ is $r_i > 1$, the corresponding $\boldsymbol{R}_i$ and $\bar{\boldsymbol{\phi}}_i$ are both $r_i \times r_i$ matrices. Defining $\boldsymbol{\Lambda}_i = \boldsymbol{R}_i\bar{\boldsymbol{\phi}}_i\boldsymbol{R}_i^{-1}$, we conclude that the corresponding $\bar{\boldsymbol{\phi}}_i$ can be estimated as the eigenvalues of $\boldsymbol{\Lambda}_i$. Specially, for those eigenvalues whose multiplicity is $r_i = 1$ in $\boldsymbol{\Gamma}(\theta)$, $\boldsymbol{R}_i$ is a 1×1 identity matrix, and, $\boldsymbol{R}_i\bar{\boldsymbol{\phi}}_i\boldsymbol{R}_i^{-1} = \bar{\phi}_i$. Finally, the time delay of k-th path can be estimated as $\hat{\tau}_k = (\angle\phi_k)N/2\pi$.

The above method of extracting the poles can be divided into two parts. Firstly, extracting θ_k and checking if there is any repeated θ_k. This can be done by computing $\frac{|\theta_{k+1}-\theta_k|}{|\theta_k|}$, If the result is less than a predefined threshold, then θ_{k+1} and θ_k are considered as identical. Then if there are no repeated θ_k, we can get $\boldsymbol{\Gamma}(\phi)$ by applying the eigenvector matrix W to $\boldsymbol{\Psi}_\phi$ i.e. $\boldsymbol{\Gamma}(\phi) = \boldsymbol{W}^{-1}\boldsymbol{\Psi}_\phi\boldsymbol{W}$. And if there are repeated θ_k, for each repeated eigenvalue θ_k, we extract the corresponding block $\boldsymbol{\Lambda}_k$ and apply EVD on $\boldsymbol{\Lambda}_k$ to estimate θ_k and ϕ_k simultaneously.

E. CONDITIONS ON THE PENCIL PARAMETER

In the process of extracting poles, the condition of $\text{rank}(\boldsymbol{U}_{s1}) = K$ and $\text{rank}(\boldsymbol{U}_{sp1}) = K$ should be satisfied. According to $\boldsymbol{D}_L$ in (21), it is found that the necessary condition for $\text{rank}(\boldsymbol{U}_{s1}) = K$ is that the number of rows of $\boldsymbol{U}_{s1}$ is not less than K, that is:

$$z_1 \times (z_2 - 1) \geq K \quad (38)$$

Similarly, the necessary condition for $\text{rank}(U_{sp1}) = K$ is:

$$z_2 \times (z_1 - 1) \geq K \quad (39)$$

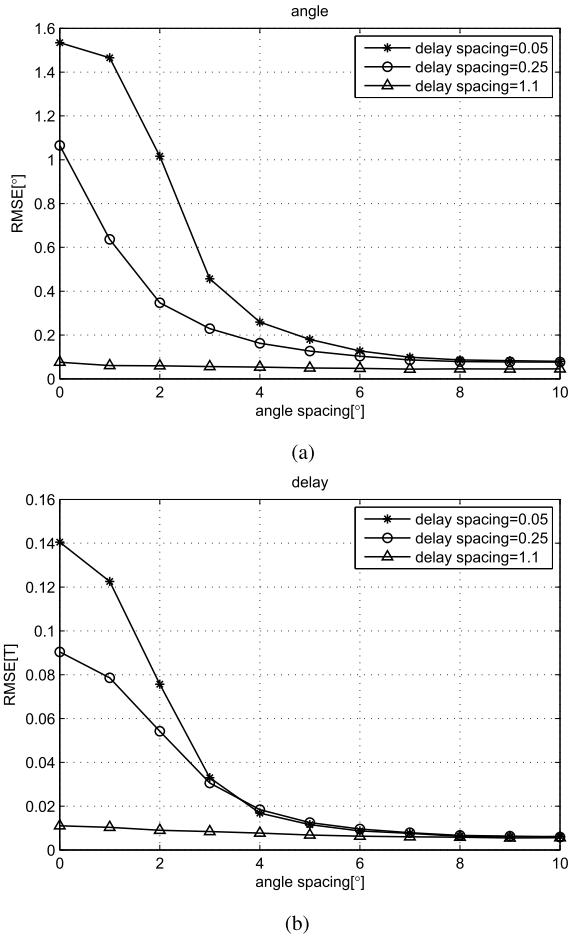

FIGURE 3. RMSE versus angle spacing. (a) RMSE of DOA versus angle spacing. (b) RMSE of time delay versus angle spacing.

Combined with (22), the conditions required for the two pencil parameters are:

$$\begin{aligned} z_1 \times (z_2 - 1) &\geq K \\ z_2 \times (z_1 - 1) &\geq K \\ (M - z_2 + 1)(N - z_1 + 1) &\geq K. \end{aligned} \quad (40)$$

In the case that the pencil parameters z_1, z_2 meet the above conditions, the values of them can be adjusted to improve the estimation performance. Intuitively, the larger the noise subspace is, the more noise component is absorbed into the noise subspace and the less noise component remains in the signal subspace [16]. In the process of DOA and TDOA estimation, only the signal subspace is used, so the larger noise subspace means the higher estimation accuracy. After the SVD in (24), a K-dimensional signal subspace spanned by $\boldsymbol{U}_s$ and a $(\min(z_1z_2, 2(M - z_2 + 1)(N - z_1 + 1)) - K)$-dimensional noise subspace spanned by U_n can be obtained. When $z_1z_2 < 2(M - z_2 + 1)(N - z_1 + 1)$, we can increase the estimation accuracy by increasing z_1, z_2 or both. Until $z_1z_2 = 2(M - z_2 + 1)(N - z_1 + 1)$ or $z_1 = (2 - \sqrt{2})(N + 1)$ and $z_2 = (2 - \sqrt{2})(M + 1)$, the noise subspace is maximized. Similarly, when $z_1z_2 > 2(M - z_2 + 1)(N - z_1 + 1)$, with

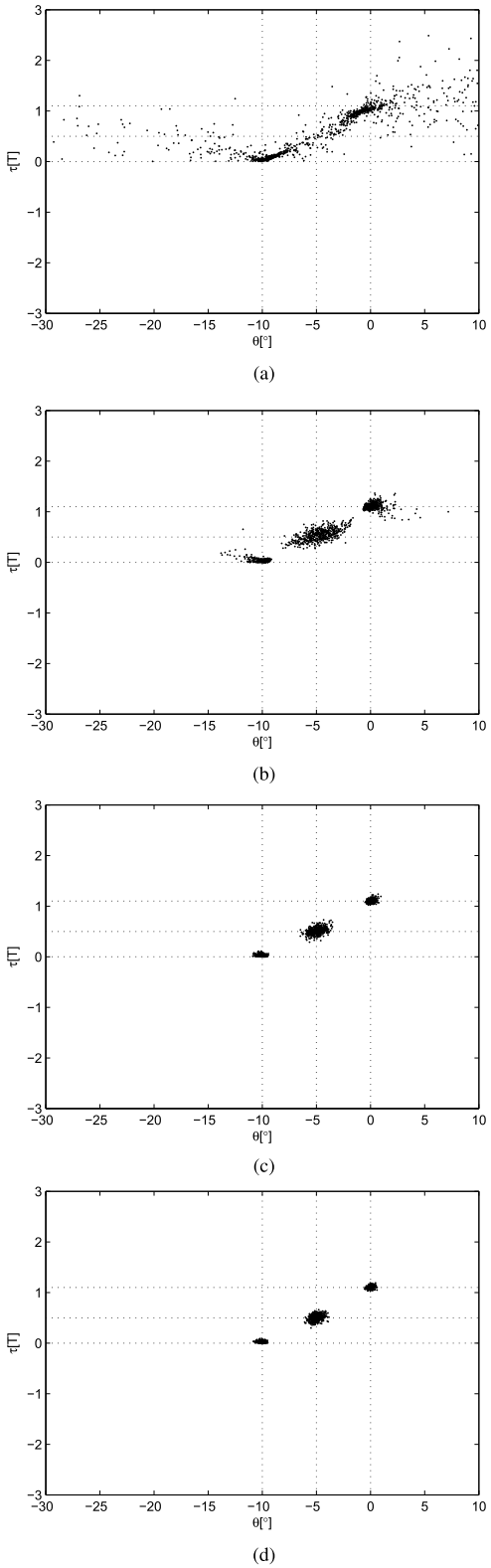

FIGURE 4. 1000 independent estimates for different values of z_1 and z_2. (a) $z_1 = 3, z_2 = 2$. (b) $z_1 = 4, z_2 = 3$. (c) $z_1 = 5, z_2 = 4$. (d) $z_1 = 6, z_2 = 5$.

the increase of $z_1 z_2$, on one hand the noise subspace will reduce which leads to the decrease of estimation accuracy, on the other hand the amount of calculation will increase.

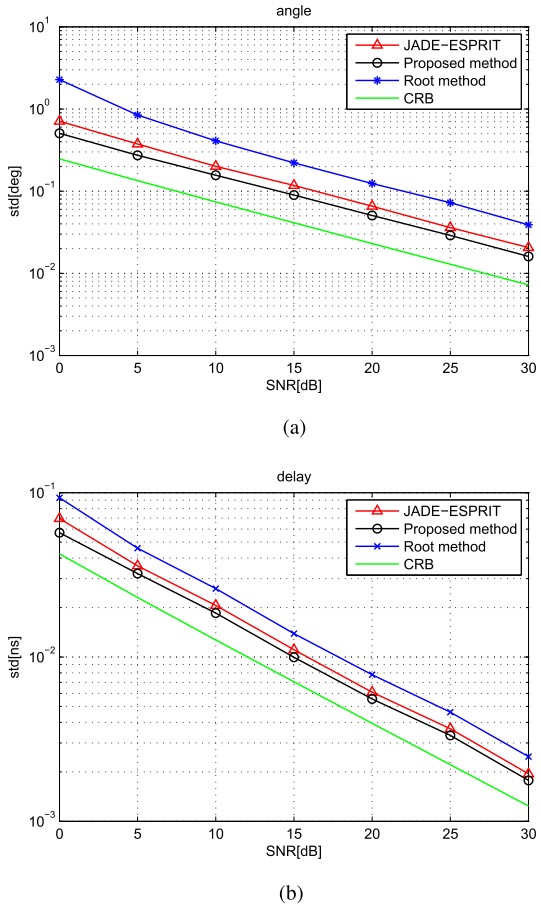

FIGURE 5. RMSE versus with SNR. (a) RMSE of DOA. (b) RMSE of time delay.

Therefore, under the condition that the amount of computation can be accepted, we can choose the value of z_1 and z_2 that are close to $\left\lceil (2-\sqrt{2})(N+1) \right\rceil$ and $\left\lceil (2-\sqrt{2})(M+1) \right\rceil$ to reduce the influence of noise.

IV. SIMULATION RESULTS

A series of simulations and analysis were carried out to show the performance of the proposed algorithm. Assuming that M-element array is a uniform linear array with half wavelength spacing. And the number of snapshots L is 40. The pulse waveform function is a truncated raised cosine pulse with a roll off factor of 0.35 because of its good attenuation characters outside the band [12], which truncated a symbol length of $N_g = 6$. The channel length is $N = 10$ and over sampling rate $P = 2$, all the results are based on 1000 Monte Carlo trials.

a) Assuming to multipath number $K = 2$, elements number $M = 8$ and keeping a constant angle and time delay value $(-10°, 0T_s)$ of the first received ray. The resolution of the algorithm can be illustrated by changing the angle and time delay of the second received ray. Fig.3 shows the variation of root-mean-square-error (RMSE) with the angular

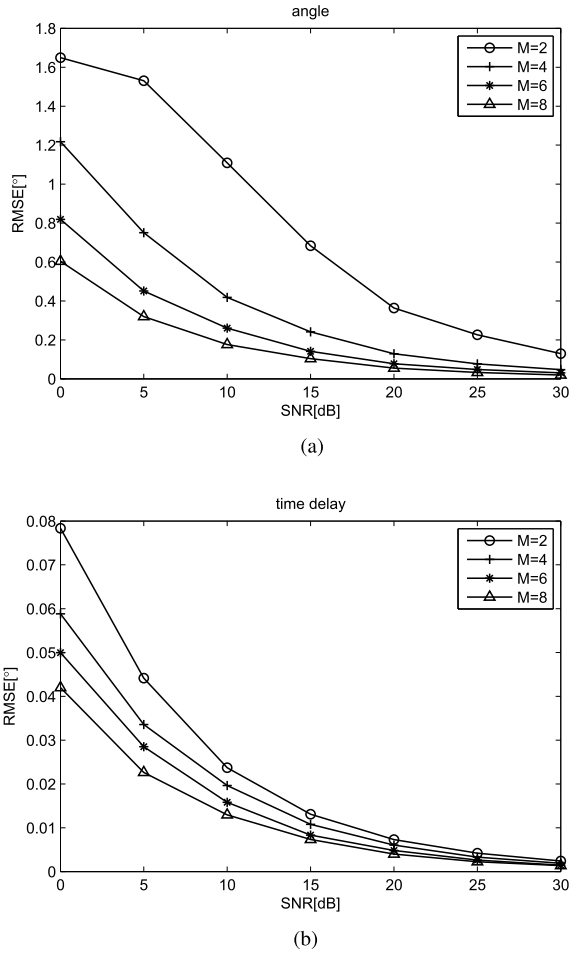

FIGURE 6. RMSE versus with SNR in different M. (a) RMSE of DOA. (b) RMSE of time delay.

spacing when the time delay interval of two received rays is $\Delta\tau$=$[0, 0.25, 1.1]T_s$. Fading coefficient is β=$[1, 0.8e^{j\pi/4}]$, Signal-to-Noise Ratio (SNR) is 20dB and other conditions are same as above. It can be seen that the estimation accuracy improve with the increasing of the angular spacing when the time delay interval of the two path is $0.05T_s$ until the angular spacing reaches 8°. When the delay interval is $1.1T_s$, the estimation accuracy does not vary with the angle spacing basically. And we can draw that the algorithm in this paper is still available when the same DOA or time delay exists in multipath.

b) In order to verify the influence of pencil parameters to the algorithm, Fig.4 compares the estimation of the DOA and TDOA under the different values of z_1 and z_2. In SNR=20dB and $M = 8$, we set a more critical case where the three incident angles and delays are $\theta = [-10°, -5°, 0°]$, $\tau = [0, 0.5, 1.1]T_s$, respectively. In the four sub-figures of Fig.4, the values of z_1 and z_2 are $(3, 2), (4, 3), (5, 4)$ and $(6, 5)$. As seen from Fig.4, with the increase of the values of z_1 and z_2, the three clusters become smaller. Just as discussed in III-E, until $z_1 = \left\lceil (2-\sqrt{2})(N+1) \right\rceil = 6$, $z_2 = \left\lceil (2-\sqrt{2})(M+1) \right\rceil = 5$ the estimation performance is best. And the estimation accuracy will decrease with the increase of z_1 and z_2, which is not show here.

c) We compares the RMSE of the angle and delay estimates of the proposed method, JADE-ESPRIT algorithm [12], the root algorithm [8] and the Cramer-Rao Bound (CRB) [11]. The multipath number is $K = 3$ and elements number of array is $M = 8$. Setting three incidence angles as $\theta = [-10°, 20°, 50°]$, with corresponding time delay of $\tau = [0, 1.1, 2.8]T_s$ and fading coefficients of $\beta = \left[1, 0.8e^{j\pi/4}, 0.6e^{j\pi/6}\right]$. Matrix pencil parameters is $z_1 = 6, z_2 = 5$. In Fig.5, it shows the RMSE of DOA and time delay of the first incident ray as an example with respect to the SNRs from 0dB to 30dB with 5dB step. As we can see, the RMSE obtained by the proposed algorithm is less than the other two algorithms, which proves that the proposed algorithm has better performance.

d) Fig.6 shows the RMSE of DOA and time delay versus SNR for the different number of sensors. The simulation condition is same to the condition mentioned in c), and the number of sensors is $M = 2, 4, 6, 8$ respectively. As expected, with the increase of the number of elements and SNR, the performance of the proposed algorithm becomes better. And this algorithm is also effective when the elements number is less than the incident signals number, see the curve of $M = 2$ in the figure.

V. CONCLUSIONS

In this paper, we propose a high resolution algorithm of joint estimate DOA and delay in multipath environment. The channel model can be obtained by Fourier transform and deconvolution of the known pulse shape. Then a 2-D matrix pencil algorithm is used to estimate and match these two parameters. The simulation results show that the proposed algorithm has higher accuracy compared with JADE-ESPRIT, and can separate the rays with the same DOA or TDOA. All simulations are carried out in a small number of snapshots, and have good performance.

ACKNOWLEDGMENT

The authors would like to thank the anonymous reviewers and the associate editor for their valuable comments and suggestions, which have greatly improved the quality of this paper.

REFERENCES

[1] G. Bartoli, R. Fantacci, D. Marabissi, and M. Pucci, "LTE-A femto-cell interference mitigation with MuSiC DOA estimation and null steering in an actual indoor environment," in *Proc. IEEE Int. Conf. Commun. (ICC)*, Budapest, Hungary, Jun. 2013, pp. 2707–2711.

[2] M. Koivisto *et al.*, "Joint device positioning and clock synchronization in 5G ultra-dense networks," *IEEE Trans. Wireless Commun.*, vol. 16, no. 5, pp. 2866–2881, May 2017.

[3] R. Amiri, F. Behnia, and H. Zamani, "Asymptotically efficient target localization from bistatic range measurements in distributed MIMO radars," *IEEE Signal Process. Lett.*, vol. 24, no. 3, pp. 299–303, Mar. 2017.

[4] L. Wan, G. Han, J. Jiang, C. Zhu, and L. Shu, "A DOA estimation approach for transmission performance guarantee in D2D communication," *Mobile Netw. Appl.*, vol. 22, no. 6, pp. 998–1009, Feb. 2017.

[5] T. Patelczyk and E. Biebl, "Implementation aspects of joint angle and delay estimation for road traffic applications," in *Proc. IEEE 6th Int. Conf. Commun. Electron. (ICCE)*, Ha Long, Vietnam, Jul. 2016, pp. 61–66.
[6] G. Villemin, C. Fossati, and S. Bourennane, "Spatio-temporal-based joint range and angle estimation for wideband signals," *EURASIP J. Adv. Signal Process.*, vol. 2013, no. 1, p. 131, 2013.
[7] M. Wax and A. Leshem, "Joint estimation of time delays and directions of arrival of multiple reflections of a known signal," *IEEE Trans. Signal Process.*, vol. 45, no. 10, pp. 2477–2484, Oct. 1997.
[8] P. Singh and P. Sircar, "Time delays and angles of arrival estimation using known signals," *Signal, Image Video Process.*, vol. 6, no. 2, pp. 171–178, Feb. 2011.
[9] D. Grenier, B. Elahian, and A. Blanchard-Lapierre, "Joint delay and direction of arrivals estimation in mobile communications," *Signal, Image Video Process.*, vol. 10, no. 1, pp. 45–54, Oct. 2014.
[10] L. Liu and H. Liu, "Joint estimation of DOA and TDOA of multiple reflections in mobile communications," *IEEE Access*, vol. 4, pp. 3815–3823, 2016.
[11] M. C. Vanderveen, C. B. Papadias, and A. Paulraj, "Joint angle and delay estimation (JADE) for multipath signals arriving at an antenna array," *IEEE Commun. Lett.*, vol. 1, no. 1, pp. 12–14, Jan. 1997.
[12] A.-J. van der Veen, C. M. Vanderveen, and A. Paulraj, "Joint angle and delay estimation using shift-invariance techniques," *IEEE Trans. Signal Process.*, vol. 46, no. 2, pp. 405–418, Feb. 1998.
[13] R. Roy, and T. Kailath, "ESPRIT—Estimation of signal parameters via rotational invariance techniques," *IEEE Trans. Acoust. Speech Signal Process.*, vol. 37, no. 7, pp. 984–995, 1989.
[14] K. Bayat and R. S. Adve, "Joint TOA/DOA wireless position location using matrix pencil," in *Proc. IEEE 60th Veh. Technol. Conf.*, Los Angeles, CA, USA, Sep. 2004, pp. 3535–3539.
[15] D. A. Bykov and L. L. Doskolovich, "Numerical methods for calculating poles of the scattering matrix with applications in grating theory," *J. Lightw. Technol.*, vol. 31, no. 5, pp. 793–801, Mar. 1, 2013.
[16] Y. Hua, "Estimating two-dimensional frequencies by matrix enhancement and matrix pencil," *IEEE Trans. Signal Process.*, vol. 40, no. 9, pp. 2267–2280, Sep. 1992.
[17] A. Gaber and A. Omar, "A study of wireless indoor positioning based on joint TDOA and DOA estimation using 2-D matrix pencil algorithms and IEEE 802.11ac," *IEEE Trans. Wireless Commun.*, vol. 14, no. 5, pp. 2440–2454, May 2015.
[18] F.-J. Chen, C. C. Fung, C.-W. Kok, and S. Kwong, "Estimation of 2-dimensional frequencies using modified matrix pencil method," in *Proc. IEEE 6th Workshop Signal Process. Adv. Wireless Commun.*, New York, NY, USA, Jun. 2005, pp. 850–854.

YU ZHENG was born in Cixi, Zhejiang, China, in 1978. He received the B.A. degree in electronics engineering from Harbin Engineering University, China, in 2000, and the M.Sc. degree in electronics engineering from the Nanjing University of Science and Technology, in 2009. He is currently pursuing the Ph.D. degree with the College of Information and Telecommunication, Harbin Engineering University. His research interests include the general area of model predictive control and radar signal processing.

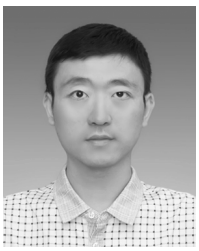

YONGZHI YU received the B.S. degree in communication engineering and the M.S. and Ph.D. degrees in signal and information processing from Harbin Engineering University, Harbin, China, in 2003, 2006, and 2009, respectively. In 2003, he joined the faculty of Harbin Engineering University, where he is currently a Lecturer with the College of Information and Communication Engineering. In 2011, he visited the University of Glasgow, Glasgow, U.K., as a Visiting Scholar. His research interests include radar signal processing, digital communications, and coding techniques applied to wireless systems.